The non-invasive Berlin Brain–Computer Interface: Fast acquisition of effective performance in untrained subjects

Benjamin Blankertz,[a,*] Guido Dornhege,[a] Matthias Krauledat,[a,b]
Klaus-Robert Müller,[a,b] and Gabriel Curio[c]

[a]Fraunhofer FIRST (IDA), Kekuléstr. 7, 12 489 Berlin, Germany
[b]Technical University of Berlin, Dept. of Computer Science, Berlin, Germany
[c]Dept. of Neurology, Campus Benjamin Franklin, Charité University Medicine Berlin, Germany

Brain–Computer Interface (BCI) systems establish a direct communication channel from the brain to an output device. These systems use brain signals recorded from the scalp, the surface of the cortex, or from inside the brain to enable users to control a variety of applications. BCI systems that bypass conventional motor output pathways of nerves and muscles can provide novel control options for paralyzed patients. One classical approach to establish EEG-based control is to set up a system that is controlled by a specific EEG feature which is known to be susceptible to conditioning and to let the subjects learn the voluntary control of that feature. In contrast, the Berlin Brain–Computer Interface (BBCI) uses well established motor competencies of its users and a machine learning approach to extract subject-specific patterns from high-dimensional features optimized for detecting the user's intent. Thus the long subject training is replaced by a short calibration measurement (20 min) and machine learning (1 min). We report results from a study in which 10 subjects, who had no or little experience with BCI feedback, controlled computer applications by voluntary imagination of limb movements: these intentions led to modulations of spontaneous brain activity specifically, somatotopically matched sensorimotor 7–30 Hz rhythms were diminished over pericentral cortices. The peak information transfer rate was above 35 bits per minute (bpm) for 3 subjects, above 23 bpm for two, and above 12 bpm for 3 subjects, while one subject could achieve no BCI control. Compared to other BCI systems which need longer subject training to achieve comparable results, we propose that the key to quick efficiency in the BBCI system is its flexibility due to complex but physiologically meaningful features and its adaptivity which respects the enormous inter-subject variability.

Introduction

The aim of Brain–Computer Interface (BCI) research is to establish a novel communication system that translates human intentions–reflected by suitable brain signals–into a control signal for an output device such as a computer application or a neuroprosthesis. According to the definition put forth at the first international meeting for BCI technology in 1999, a BCI "must not depend on the brain's normal output pathways of peripheral nerves and muscles" (Wolpaw et al., 2000).

There is a huge variety of BCI systems (see Pfurtscheller et al., 2005; Wolpaw et al., 2002; Kübler et al., 2001; Dornhege et al., 2007b; Curran and Stokes, 2003). BCI systems relying on intentional modulations of evoked potentials can typically achieve higher information transfer rates (ITRs) than systems working on unstimulated brain signals (cf. Cheng et al., 2002; Kaper and Ritter, 2004). On the other hand, with evoked potential BCIs the user is constantly confronted with stimuli, which could become exhaustive after longer usage. Furthermore, some patient groups might not be able to properly focus their gaze and thus such a system will not be a reliable means for their communication when visual evoked potentials are employed.

One of the major challenges in BCI research is the huge inter-subject variability with respect to spatial patterns and spectrotemporal characteristics of brain signals. In the operant conditioning variant of BCI, the subject has to learn the self-control of a specific EEG feature which is hard-wired in the BCI system (see e.g., Elbert et al., 1980; Rockstroh et al., 1984; Birbaumer et al., 2000). An alternative approach tries to establish BCI control in the opposite way: while using much more general features, the system automatically adapts to the specific brain signals of each user by employing advanced techniques of machine learning and signal processing (e.g., Müller et al., 2001; Haykin, 1995; and more specifically with respect to BCI: Blankertz et al., 2004, 2006c,d; Müller et al., 2003, 2004).

The Graz BCI group introduced the common spatial pattern (CSP) algorithm (spatial filters that are optimized for the discrimination of different condition, cf. Common spatial pattern (CSP)

* Corresponding author. Fax: +49 30 6392 1805.
  E-mail address: benjamin.blankertz@first.fraunhofer.de (B. Blankertz).
  Available online on ScienceDirect (www.sciencedirect.com).

analysis) for the use in BCI systems (Ramoser et al., 2000) and reported in (Guger et al., 2000a) results from a feedback study with a CSP-based BCI operating on a 27 channel EEG. The feedback study encompassed 6 sessions on 4 days for each of three subjects that were experienced with BCI control. Nevertheless the result for two out of three subjects was at chance level in the first feedback session and reasonable BCI control was only obtained from the 2nd feedback session on. The feedback application did not allow to explore what information transfer rates could be obtained because it relied on a synchronous design where each binary decision needed 8 s, limiting the highest possible ITR to 7.5 bits per minute (bpm) at a theoretical accuracy of 100%. In a more recent publication (Krausz et al., 2003) 4 patients with complete or partial paralysis or paresis of their lower limbs were trained to operate a variant of the Graz BCI that uses band power features of only 2 bipolar channels. As feedback application, a basket game was used in which the subject controls the horizontal position of a ball that falls downward at constant speed. The aim in this application is to hit one of two basket targets at the bottom of the screen. On the second and third day the maximum ITR of 6–16 runs of 40 trials each for the 4 subjects was between 3 and 17.2 bpm (mean 9.5 ± 5.9).

A study from the Wadsworth BCI group (McFarland et al., 2003) investigates the influence of trial duration and number of targets on the ITR in their BCI system that uses operant conditioning for letting the users learn to modulate the amplitude of sensorimotor rhythms. Eight subjects (2 patients, one spinal injury at c6 and one cerebral palsy) trained over several months to operate a BCI application similar to the basket game described above, but with vertical cursor control and a variable number of target fields. The average ITR from 8 runs of 20 to 30 trials for the 8 subjects was between 1.8 and 17 bpm (mean 8.5 ± 4.7) at the individual best number of targets. In a more recent study in cooperation with the BCI group in Tübingen (Kübler et al., 2005) a similar methodology was successfully used with 4 patients suffering from Amyotrophic Lateral Sclerosis (ALS). This was the first study demonstrating that ALS patients are capable of voluntarily modulating the amplitude of their sensorimotor rhythms to control a BCI.

Based on offline results, del Millán et al. (2002) suggest to use a local neural classifier based on quadratic discriminant analysis for the machine learning part. Using this system asynchronously in an online feedback with three classes (left/right-hand motor imagery and relax with eyes closed) three subjects were able after a few days of training to achieve an average correct recognition of about 75% whereas the wrong decision rates were below 5%. In del Millán and Mouriño (2003) it was reported that with this system a motorized wheelchair and a virtual keyboard could be controlled. In the latter case trained subjects were able to select a letter every 22 s. In a preliminary study the best subject was reported to be able to do selections every 7 s. Note that brain signals for one class were produced by closing the eyes.

Here we demonstrate how an effective and fast BCI performance can be realized even for untrained subjects by use of modern machine learning techniques (cf. Algorithms and procedures and Methodological and technical details).

Materials and methods

Neurophysiology and features

According to the 'homunculus' model, as described by Jasper and Penfield (1949), for each part of the human body there exists a corresponding region in the primary motor and primary somatosensory area of the neocortex. The 'mapping' from the body part to the respective brain areas approximately preserves topography, i.e., neighboring parts of the body are represented in neighboring parts of the cortex. For example, while the feet are located close to the vertex, the left hand is represented lateralized (by about 6 cm from the midline) on the right hemisphere and the right hand almost symmetrically on the left hemisphere.

Macroscopic brain activity during resting wakefulness contains distinct 'idle' rhythms located over various brain areas, e.g., the μ rhythm can be measured over the pericentral sensorimotor cortices in the scalp EEG, usually with a frequency of about 10 Hz (Jasper and Andrews, 1938). Furthermore, in electrocorticographic recordings Jasper and Penfield (1949) described a strictly local β rhythm at about 20 Hz over the human motor cortex. In non-invasive scalp EEG recordings the 10 Hz μ rhythm is commonly mixed with the 20 Hz-activity. Basically, these rhythms are cortically generated; while the involvement of a thalamo-cortical pacemaker has been discussed since the first description of EEG by Berger (1933), Lopes da Silva (da Silva et al., 1973) showed that cortico-cortical coherence is larger than thalamo-cortical pointing to a convergence of subcortical and cortical inputs.

The moment-to-moment amplitude fluctuations of these local rhythms reflect variable functional states of the underlying neuronal cortical networks and can be used for brain–computer interfacing. Specifically, the pericentral μ and β rhythms are diminished, or even almost completely blocked, by movements of the somatotopically corresponding body part, independent of their active, passive, or reflexive origin. Blocking effects are visible bilateral but with a clear predominance contralateral to the moved limb. This attenuation of brain rhythms is termed event-related desynchronization (ERD) (see Pfurtscheller and Lopes da Silva, 1999; Pfurtscheller et al., 2006).

Since a focal ERD can be observed over the motor and/or sensory cortex even when a subject is only imagining a movement or sensation in the specific limb, this feature can well be used for BCI control: the discrimination of the imagination of movements of left hand vs. right hand vs. foot can be based on the somatotopic arrangement of the attenuation of the μ and/or β rhythms. To this end, spatio-spectral filters to improve the classification performance of the CSP algorithm were suggested (e.g., Lemm et al., 2005).

A complementary EEG feature reflecting imagined or intended movements is the lateralized Bere-itschaftspotential (readiness potential, RP), a negative shift of the DC-EEG over the activated part of the primary motor cortex (Blankertz et al., 2003, 2006a,c). The RP feature was used in combination with co-localized ERD features and showed encouraging results in offline BCI classification studies (Dornhege et al., 2004a,b, 2007c).

Experimental setup

Ten subjects (all male; 1 left handed; age 26–46 years, all staff members at the two involved institutions) took part in a series of feedback experiments. None of the subjects had extensive training with BCI feedback: two subjects had no prior experience with BCI feedback, four subjects had one session with (an earlier version of) BBCI feedback, three subjects had 4 sessions of BBCI feedback before, and one subject had previously 2 sessions of cursor control feedback and about 4 sessions of different BBCI feedback. See the discussion of the influence of the prior feedback experience in Impact of previous feedback sessions.

Brain activity was recorded with multi-channel EEG amplifiers (Brain Products GmbH, Germany) using 128 channels (64 for subjects 7–10) band-pass filtered between 0.05 and 200 Hz and sampled at 1000 Hz. For all results in this paper, the signals were subsampled at 100 Hz. Additionally surface EMG at both forearms and the right leg, as well as horizontal and vertical EOG signals, were recorded. Those signals were exclusively used to check the absence of target-related muscle activity or eye movements (see Investigating the dependency of BCI control). They have not been used for generating the feedback. Subjects sat in a comfortable chair with arms placed on armrests. All recordings for one individual subject were recorded on the same day.

Calibration sessions

All experiments contain a so called calibration session in which the subjects performed mental motor imagery tasks, guided by visual command stimuli. Thereby labeled examples of brain activity can be obtained during the different mental tasks. These recorded single trials were then used to train a classifier by machine learning techniques which was applied online in the feedback sessions to produce a feedback signal for (unlabeled) continuous brain activity. Note that the 'calibration sessions' are only used to generate examples to calibrate the classifier, not to train the subject.

In the calibration session visual stimuli indicated which of the following 3 motor imageries the subject should perform: (L) left hand, (R) right hand, or (F) right foot. Target cues were visible on the screen for a duration of 3.5 s, interleaved by periods of random length, 1.75 to 2.25 s, in which the subject could relax.

There were two types of visual stimulation: (1) targets were indicated by letters appearing at a central fixation cross and (2) a randomly moving small rhomboid with either its left, right, or bottom corner filled to indicate left or right hand or foot movement, respectively. Since the movement of the object was independent from the indicated targets, target-uncorrelated eye movements are induced. This way the classifier becomes robust against changes in the brain signals caused by eyes movements. For seven subjects 2 sessions of both types were recorded, while from the other three subjects 1 session of type (1) and 3 sessions of type (2) were recorded. Overall 140 trials for each imagery class have been recorded.

Feedback sessions

After the calibration sessions were recorded, the experimentor screened the data to adjust subject-specific parameters of the data processing methods (see Learning for calibration data and Selection of hyperparameters). Then he identified the two classes that gave best discrimination and trained a binary classifier as described in Algorithms and procedures. The third class was not used for feedback. In cases where the cross-validation (cf. Validation) predicted a reasonable performance, the subject continued with three types of feedback sessions. Two have an asynchronous protocol[1],

---

[1] These feedback applications fall between the categories 'synchronous' and 'asynchronous'. While there are visual cues indicating the target, the time point at which the decision is taken is not fixed beforehand but rather depends on the brain signals of the user. If the user is in idle state the classifier output should be small in magnitude such that the cursor stays in the center and does not actuate a selection. In contrast to feedbacks with fixed trial length we call this type of feedback 'asynchronous' albeit a systematic evaluation of the idle state feature was not done.

while the last is synchronous. Since most timing details were individually adapted for each subject, we will here only report the range in which those changes occurred. In all feedback scenarios, we arranged the display according to the selected paradigms, in particular we wanted to make the movement most intuitive for the subjects. If the selected classes were "right hand" and "right foot", then a vertical movement was more intuitive than a horizontal one. For reasons of legibility, only the setup for the horizontal movement will be described in the following sections.

Position controlled cursor. The first type of feedback presented to the subjects consisted of the control of a cursor in one-dimensional (i.e., horizontal) direction. Items on the screen included the cursor in form of a red cross of approximately 3 cm width, two targets in form of grey rectangles of 15 cm height and 3 cm width (one at each lateral side of the screen) and a counter at the top left corner of the screen, indicating the respective numbers of successful and unsuccessful trials. In the middle, a light gray rectangle of 20 cm width denoted a designated central area, see Fig. 1.

The display was refreshed at 25 fps, and with every new frame at time t_0, the cursor was updated to a new position $(p_{t_0}, 0)$ calculated from the classifier output $(c_t)_{t \le t_0}$, according to the formula

$$p_{t_0} = s \left(\frac{1}{n} \sum_{t=t_0-n+1}^{t_0} c_t - b \right), \tag{1}$$

where scaling factor s, bias b and averaging length n were manually adjusted during a calibration session. We then restrict the range of the above expression to the interval $[-1, 1]$ and translated this interval to horizontal positions on the screen.

The cursor was visible and controllable throughout the whole run. At the beginning of each trial, the cursor was a black dot and had to be moved into the central area of the screen (Fig. 1) where the shape of the cursor changed to a cross. After that the task was to steer the cursor into the highlighted target by imagining the corresponding unilateral hand movements.

Once a target (non-target) was hit by the cursor, it was colored green (or red) to show the success (or failure) of the performance, and the cursor turned to dot shape again. As long as the cursor had the dot shape, no selections (neither hits nor misses) could be made. This strategy prevented unintended multiple activations of the same target. As an additional information for the subjects, a 1 cm stripe at the outermost section of the targets was colored blue or gray to indicate whether or not this side was going to be the next target (preview). Each run consisted of 25 trials of this kind.

Rate controlled cursor. The setup for the second type of feedback was similar to the previous one, only the control strategy for the cursor was slightly modified. In this setting, the cursor was moving in a "relative" fashion, meaning that with every new frame, the new position p_{t_0} was the old position p_{t_0-1}, shifted by an amount proportional to the classifier output:

$$p_{t_0} = p_{t_0-1} + s \left(\frac{1}{n} \sum_{t=t_0-n+1}^{t_0} c_t - b \right). \tag{2}$$

In other words, in this setting, the first derivative (i.e., direction and speed) of the cursor position was controlled rather than its absolute position.

At the beginning of each trial, the cursor was set to the central position and was kept fixed for 750–1000 ms before it could start moving.
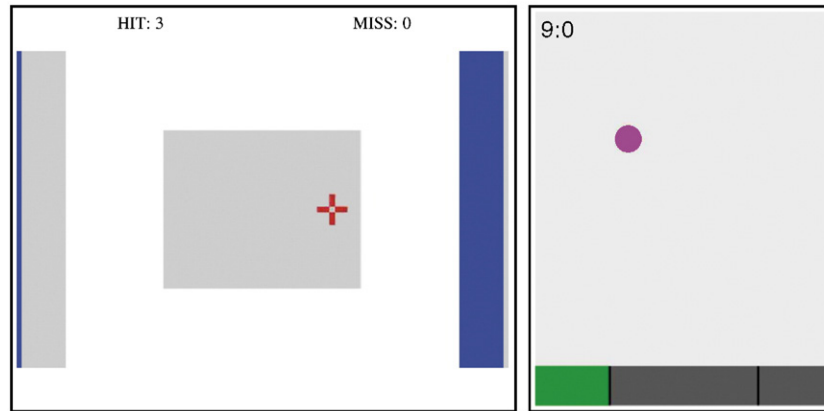
Fig. 1. The setup of the feedback session. Left panel—"cursor control": in this situation, the cursor is active and the right rectangle is marked as the current target. The stripe on the left side indicates that after the current target, the left rectangle will be highlighted as target (preview). Right panel—"basket game": the subject controls the horizontal position of a ball that falls downward at constant speed. The aim is to hit the green colored one of three baskets at the bottom of the screen.

Basket game. Here the scene consisted of three targets, gray rectangles at the bottom of the screen of approximately 3 cm height, and a counter at the upper left of the screen, which showed the number of successful and unsuccessful trials. The two outer rectangles were smaller than the middle one to account for the fact that they were easier to hit. In each trial, one of the targets was highlighted in blue, and the subject was trying to direct a cursor in the form of a magenta ball into this target. The cursor appeared at the top of the screen and was held there for 500–750 ms. Then it was moving down at a fixed rate such that it reached the bottom 1200–3000 ms (according to the subject's choice) after its release. The subjects were able to control the horizontal position of the cursor by imagining strategies as explained above. In this manner, they could try to hit the intended target when the cursor reached the bottom line. After the completion of a trial, the hit basket was highlighted green or red, according to the success of the trial. The next trial began 250 ms after hitting the target.

This feedback was similar to those described by McFarland et al. (2003) and Krausz et al. (2003) (cf. Introduction) but here, as mentioned above, we changed the sizes of the targets according to the difficulty to reach them.

Manual calibration

In our very first feedback experiments we realized that the initial classifier was behaving suboptimal. Thus we introduced a calibration phase at the beginning of the feedback sessions in which the subject controlled the cursor freely and the experimentor adjusted the bias and the scaling of the classifier (b and s in Eqs. (1) and (2)). Our investigations show that this adjustment is needed to account for the different experimental and mental conditions of the more demanding feedback situation when compared to the calibration session (cf. Krauledat et al., 2006; Shenoy et al., 2006).

Algorithms and procedures

Machine learning techniques allow to learn from calibration data optimized parameters such as (spatial and spectral) filter coefficients, separation of the class distributions, and hyperparameters of all involved methods which are needed for the online translation algorithm. Here, some of the hyperparameters that allow to in-

corporate neurophysiological knowledge have been selected semi-automatically. In this section we give an overview of the following two processes: (1) learning from calibration data, and (2) translating online brain signals to a control signal (see Methodological and technical details for details). For completeness we also summarize the Common Spatial Pattern algorithm, which is an essential part of (1).

Common spatial pattern (CSP) analysis

The common spatial pattern (CSP) algorithm (Fukunaga, 1990) is highly successful in calculating spatial filters for detecting ERD/ERS effects (see Koles and Soong, 1998) and for ERD-based BCIs (see Guger et al., 2000b) and has been extended to multi-class problems in (Dornhege et al., 2004a). Given two distributions in a high-dimensional space, the CSP algorithm finds directions (i.e., spatial filters) that maximize variance for one class and that at the same time minimize variance for the other class. After having bandpass filtered the EEG signals in the frequency domain of interest, high or low signal variance reflects a strong, respectively a weak (attenuated), rhythmic activity. Let us take the example of discriminating left hand vs. right hand imagery. According to Neurophysiology and features, if the EEG is first preprocessed in order to focus on the μ and β band, i.e., bandpass filtered in the frequency range 7–30 Hz, then a signal projected by a spatial filter focussing on the left hand area is characterized by a strong motor rhythm during the imagination of right hand movements (left hand is in idle state), and by an attenuated motor rhythm if movement of the left hand is imagined. This can be seen as a simplified exemplary solution of the optimization criterion of the CSP algorithm: maximizing variance for the class of right hand trials and at the same time minimizing variance for left hand trials. Additionally the CSP algorithm calculates the dual filter that will focus on the spatial area of the right hand in sensor space. Moreover a series of orthogonal filters of both types can be determined.

For the technical details the reader is referred to Fukunaga (1990), Ramoser et al. (2000), and Lemm et al. (2005). As result the CSP algorithm outputs a decomposition matrix W and a vector of corresponding eigenvalues. The interpretation of W is two-fold: the rows of W are the stationary spatial filters, whereas the columns of W^{-1} can be seen as the common spatial patterns, i.e., the time-

invariant EEG source distribution vectors. Each eigenvalue indicates the importance of the corresponding filter for the discrimination tasks.

CS patterns can be used to verify neurophysiological plausibility of the calculated solution, while the filters typically incorporate an intricate weighting which is needed to project out artifacts and noise sources and to optimize discriminability (see Fig. 2) The patterns are much smoother and have a broad focus, while the focus of the filters is much more localized and either has a bipolar structure or the focus is surrounded by areas that are weighted weaker but with the opposite sign. This way, influences from other areas like artifacts or non task-relevant fluctuations (ongoing activity resp. noise) are attenuated.

Recently efficient extensions of CSP for multiclass settings (Dornhege et al., 2004a) as well as optimized spatio-temporal filter extensions of CSP have been proposed (Lemm et al., 2005; Dornhege et al., 2006; Tomioka et al., 2006, in press).

Classification with LDA

The linear discriminant analysis (LDA) is obtained by deriving the classifier that minimizes the risk of misclassification under the assumption that the class distributions obey known Gaussian distributions with equal covariances. Denoting the common covariance matrix by Σ and the class means by μ_l ($l = 1, 2$) the decision function of LDA is given by

$$x \rightarrow 1.5 + 0.5 * \left(w^\top \left(x - \frac{1}{2} (\mu_1 + \mu_2) \right) \right),$$

where $w = \Sigma^{-1}(\mu_2 - \mu_1)$.

Learning from calibration data

The basic idea is to extract spatial filters that optimize the discriminability of multi-channel brain signals based on ERD effects of the (sensori-) motor rhythms, then to calculate the log band power

in those surrogate channels and finally to find a separation of the two classes (mental states) in the feature space of those log band power values. This process involves several parameters that are individually chosen for each subject, as described in Selection of hyperparameters.

1) From the three available classes, only event markers of the two classes with better discriminability are retained.
2) The raw EEG time series are band-pass filtered with a butterworth IIR filter of order 5 (frequency band subject-specific chosen, see Selection of hyperparameters).
3) Trials are constructed from the filtered EEG signals for each event marker representing a specific interval relative to the time point of visual cues, typically 750 to 3500 ms.
4) CSP is used to find 3 spatial filters per class by applying the algorithm to the trials classwise con-catenated along time. From those 6 filters some were selected according to the neurophysiological plausibility of the corresponding patterns, e.g., when exhibiting typical somatotopic pericentral foci.
5) Variance was calculated for each of the CSP channels (band power) and the logarithm was applied to yield a feature vector for each trial.
6) The LDA classifier was used to find a linear separation between the mental states. Note that this classification process can in principle be enhanced by using more complex classifiers (Müller et al., 2003).

Online translation algorithm

In the online application a new feedback output was calculated every 40 ms (resp. 4 sample points) per channel. The continuously incoming EEG signals were processed as follows:

1) The EEG channels were spatially filtered with the CSP filter matrix W that was determined from the calibration data. The
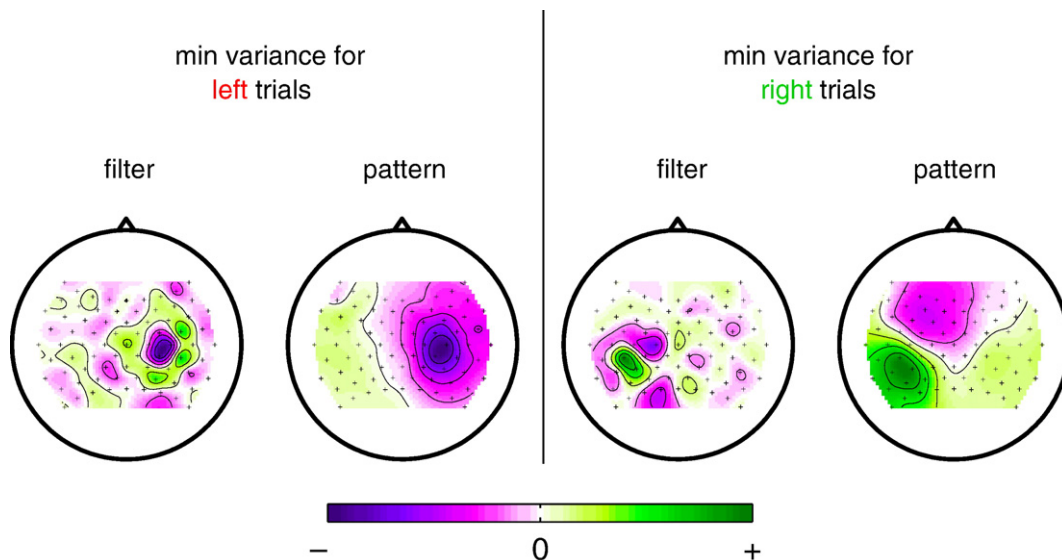

Fig. 2. The common spatial pattern (CSP) algorithm determines spatial structures which represent the optimal discrimination between two classes with respect to variance. The patterns illustrate how the presumed sources project to the scalp. They can be used to verify neurophysiological plausibility. The filters are used to project the original signals. They resemble the patterns but their intricate weighting is essential to obtain signals that are optimally discriminative with respect to variance. These two CSP filters were calculated from the calibration data of subject *aa* and have been used for feedback. Generally in this study 3 patterns/filters of each type were calculated. Neurophysiologically unplausible pattern/filter pairs were discarded from the use in online feedback.

result were 2 to 6 channels, depending on how many CSP filters were chosen.

2) The 4 new data points per channel were spectrally filtered with the chosen band-pass filter. The initial conditions of the filter are set to the final conditions of the filtering of the previous block of data. Accordingly the result of the online frequency filtering is the same as the offline forward filtering of the complete signals.

3) From the most recent interval (of given length) the log-variance was calculated in each CSP channel.

4) Feature vectors are projected perpendicular to the separating hyperplane of the LDA classifier.

5) The classifier output is scaled and a bias is added (s and b in Eqs. (1) and (2)).

6) Several consecutive outputs are averaged giving a smoother control signal (n in Eqs. (1) and (2), subject's choice).

Note that the ordering of spectral and spatial filtering was changed from the calibration to the apply phase. This is possible due to the linearity of those operations and considerably reduces computing time, since the number of channels that are to be filtered is reduced from about 100 (original EEG channels) to at most 6 (CSP channels).

Methodological and technical details

Validation

A validation was used to estimate the generalization error of the classifier with respect to the data of the calibration sessions. To this end we used a 3 times 5-fold cross-validation, i.e., for 3 repetitions all samples were partitioned into 5 parts, each of which was used as test set once, while the other 4 were used for training. Thus, 15 test set errors were determined and averaged. Since the CSP algorithm uses class label information, the calculation of the CSP filters has to be performed within the cross-validation on samples of the respective training set and the spatial filters are applied to the samples of the test set. That means for a 3 times 5-fold cross-validation the CSP algorithm is executed 15 times. The estimated generalization errors of all 3 binary class combinations are used to select the best discriminable pair of imagery conditions. In debatable cases also the subject was asked what he would rather use for control paradigm.

Selection of hyperparameters

The selection of the parameters in the calibration procedure (cf. Learning for calibration data) was done semi-automatically based on class-wise averaged plots of the spectra, of the ERD curves and of the respective r^2-values. The r^2-coefficient reflects how much of the variance in the distribution of all samples is explained by the class affiliation. It is the squared bi-serial correlation coefficient r:

$$X_r := \frac{\sqrt{N^+ \cdot N^-}}{N^+ + N^-} \frac{\text{mean}(X^-) - \text{mean}(X^+)}{\text{std}(X^+ \cup X^-)}, \quad X_{r^2} := X_r^2$$

where X^+ and X^- are the samples of class 1 and 2, respectively, and N^+ and N^- are the numbers of samples (see also Dornhege et al., 2007c; Müller et al., 2004). Whenever the sign of the difference was important, we multiplied the r^2-value with the sign of the r-value ('signed r^2-value'). Additionally the generalization error (cf. Validation) was used as indicator for good parameter values. A

visualization of the CSP analysis as shown in Fig. 2 was used to decide which CSP filters are to be used and which are to be dropped.

Selection of parameters in the feedback application

At the very beginning of the feedback sessions an exploratory phase "position controlled cursor" was performed during which experimenter and subject found out interactively which values for the meta-parameters of the feedback application were most convenient for the subject. In the first step the bias and the scaling of the classifier (b and s in Eqs. (1) and (2)) were fine tuned. The length of the window used in online classification was typically chosen between 500 and 1000 ms and the number of averaged classifier outputs was left at the default value 8. Subject aa wanted to have a more immediate feedback and chose 300 ms and 5 (effectively used for one classifier output were 5 windows of length 300 ms with a step size of 40 ms, i.e., an interval of 460 ms length). For the basket feedback, subjects could choose how fast the ball was falling down.

Results

For three subjects the combination *left* vs. *right* was found optimal, for four subjects *left* vs. *foot* and for the remaining two subjects right vs. foot (the criterium for selecting a binary pair of tasks was the discriminability of the corresponding classes of brain signals which have been acquired in the calibration measurement, see Feedback sessions and Validation). For one subject no sufficient separation was achieved (see Investigation the failure).

Neurophysiological outcome

The neurophysiological properties of the EEG of the successful subjects are summarized in Fig. 3. The brain signals of subject *au* in whom no sufficiently discriminable properties were found are discussed in Investigation the failure.

The spectra shown in the top row of Fig. 3 together with the color coded r^2-values have been used to select for each subject a frequency band (gray shading in the spectra) that exhibits good discrimination between two motor imagery tasks. This includes for all nine subjects the μ-band around 10 Hz, and extends up to the higher β-band for 6/9 subjects, thereby implementing an individually optimized passband for every subject. The second row shows the average amplitude envelope of that frequency band with 0 being the time point of the command stimulus presentation in the calibration measurement. These curves demonstrate the ERD/ERS that was caused by the ensuing motor imagery. Spectra and amplitude envelope curves were calculated from that Laplacian filtered channel that gave highest r^2-values for spectral differences. All these channels were found at the 'classical' topographic positions over pericentral hand or foot motor representations, notably with slight but significant individual deviations, e.g., for hand movements, from the standard 10–20 positions C3/4 to adjacent non-standard positions CP4 (subject *av*) or CCP5 (subject *aa*). This need for tailoring an individually optimized spatial information sampling was further corroborated by exploiting the full data from the 128-channel EEG imaging: these scalp maps reveal the spatial distribution of log band power[2] within the chosen frequency band for the two classes that were chosen to train the classifier. The top scalp map series (row 3) shows the log band power averaged over

---

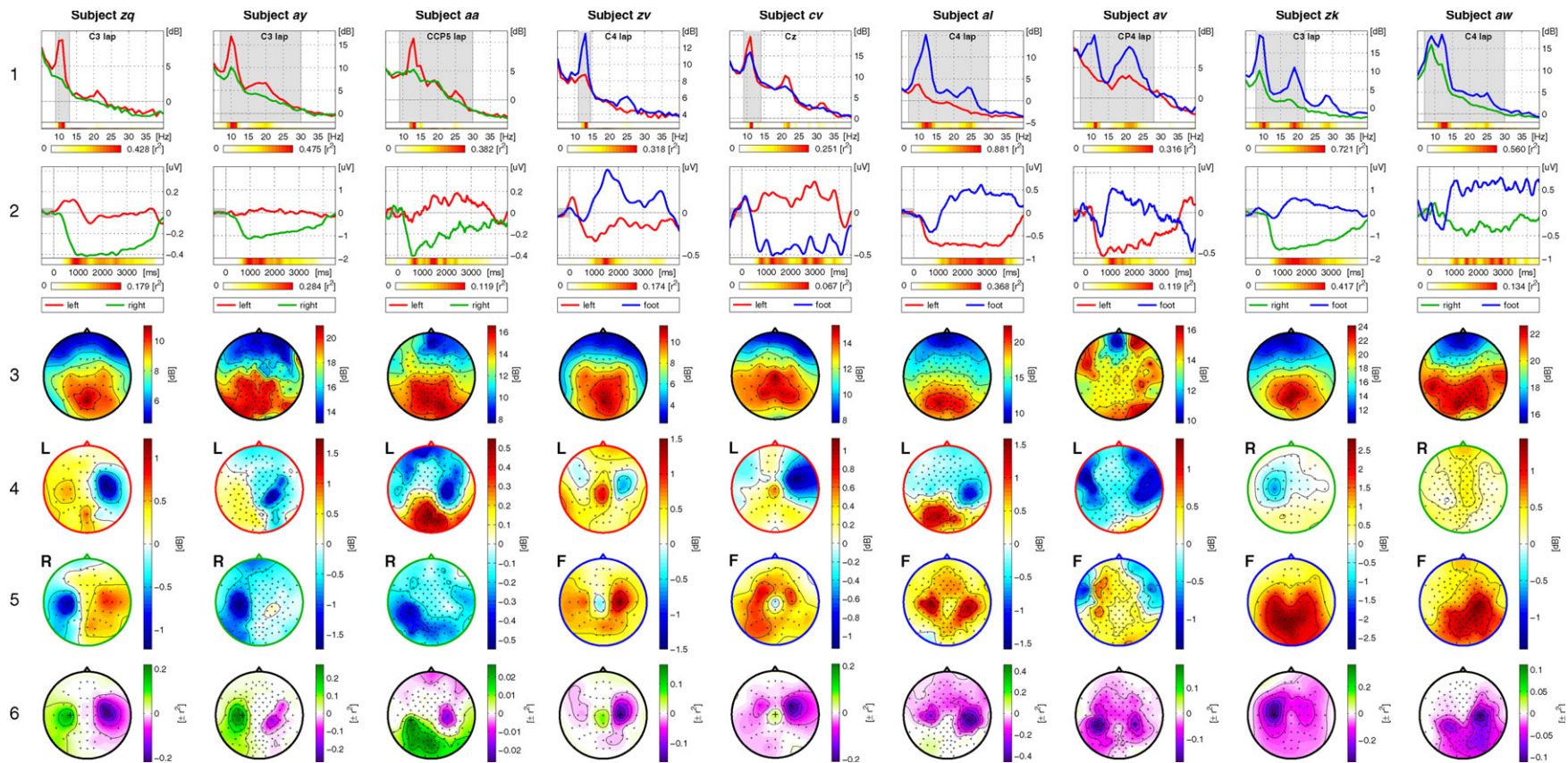[2] We transform band power to dB by applying 10 log10 to it.

Fig. 3. The first row displays the averaged spectra of the two motor imagery tasks (red: left hand, green: right hand; blue: right foot) in the calibration measurement that have been used to train the classifier. The r^2-values of the difference between those conditions are color coded and the frequency band that as been chosen is shaded gray. The second row shows the average amplitude envelope of that frequency band with 0 being the time point of stimulus presentation in the calibration measurement. The top scalp maps (row 3) show the log power within the chosen frequency band averaged over the whole calibration measurement. The fourth and fifth row display the log band power difference topographies of the particular motor imagery tasks (indicated by L, R, or F, respectively) minus the global average shown in row 3. The bottom row (6) displays the r^2-values of the difference (row 4 minus row 5) between the individually chosen motor imagery tasks as scalp map.

the whole calibration measurement. Notably, this is not a rest condition, rather it serves as reference for the specific imagery-related modulations in the calibration measurement (the pauses between motor imagery intervals were too short for having examples of a true rest condition). The fourth and fifth rows show the log band power during the execution of the two motor imagery tasks relative to the reference in row 3. The respective imagery class is indicated by the juxtaposed letters L, R, or F indicating left/right hand, or foot motor imagery, respectively. The bottom row (6) displays the signed r^2-values of the difference between the two chosen motor imagery tasks as scalp map. The difference is calculated first class (fourth row) minus second class (fifth row), i.e., green indicates more power in the first condition than in the second condition while magenta indicates the opposite relation. Whether, say, magenta coloring is caused by a desynchronization in the first condition or a synchronization in the second condition, or a combination of both cannot be decided from those maps.

The topographies of the reference condition (top scalp maps, row 3) look quite similar for all subjects with a dominating occipital/parietal α rhythm. For the motor imagery conditions we essentially expected two effects: regularly, an ERD over the sensorimotor area corresponding to the limb for which motor imagery was performed (Pfurtscheller and Lopes da Silva, 1999), and, potentially, an ERS over flanking sensorimotor areas, possibly reflecting an 'surround inhibition' enhancing focal cortical activation (see Neuper and Pfurtscheller, 2001; Pfurtscheller et al., 2006). With respect to imagination of hand movements, most subjects exhibit an ERD over the contralateral hand area. In subject *av* the ERD is also present ipsilaterally. Subjects *zv* and *cv* show also an ERS over the foot area during left hand imagery. Conspicuously, for foot motor imagery mainly an ERS over the hand areas is observed, and only 2/6 subjects (*zv*, *cv*) exhibited also a relative ERD over the foot area. This is further evidence for the necessity to tailor individually classifiers also with respect to textbook expectations of ERD/ERS

physiology, as implemented in the adaptive BBCI approach which does not enforce a priori hypotheses on the direction of power changes in the spectrally optimized passbands. The overall importance of these co-effective optimization steps becomes evident when noting that the relative difference during motor imagery compared to the reference is smaller by about factor 10 than the log band power during the reference condition.

An important result is that the r^2-topographies which display those areas that significantly discriminate the two motor imagery conditions are very clearly restricted to the involved areas of the sensorimotor cortices. Only for subject *aa* the area showing the ERD during right hand imagery extends unexpectedly to occipital regions. Nevertheless, the CSP filters that have been identified for this subject through the adaptive BBCI approach are exclusively focused on sensorimotor areas which provide the critical information for the differential motor aspect of the imagery task, as shown in Fig. 2.

Fig. 4 demonstrates that the optimized CSP filters enhance the discriminability of the brain signals. For subjects *aw* and *cv*, one of the selected CSP filters is displayed as scalp map. Plots on the right show the spectra calculated from CSP filtered brain signals.

For subject *aw* the filter extracts the signal from the sensorimotor area of the right hand and the corresponding spectrum indicates an ERD for right hand and an ERS for foot motor imagery (cf. also Fig. 3, row 2). Note that not only the peak r^2-value is increased from 0.560 (best Laplacian filtered channel, cf. Fig. 3) to 0.835, but also the non-discriminative peak at 9 Hz is filtered out almost completely. For subject *cv* the filter focuses on the foot area and the corresponding spectrum indicates an ERD for foot and an ERS for left hand motor imagery (cf. also Fig. 3, row 2). Here the peak r^2-value was increased from 0.251 to 0.399.

For each subject, from 2 up to 6 CSP filters were selected. A linear classifier then combines the log band power estimates in the CSP filtered channels to a one-dimensional output signal. Fig. 2
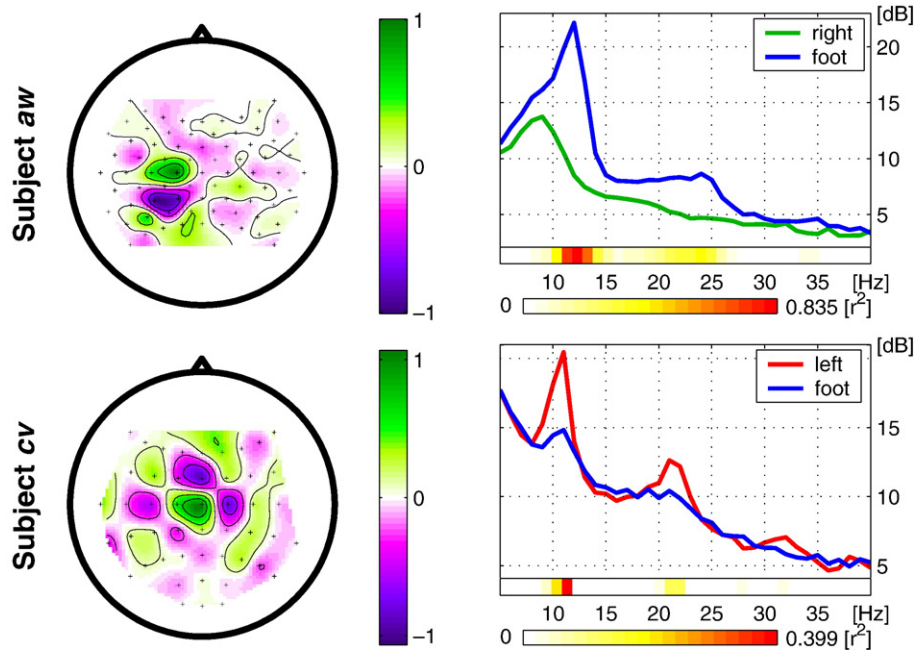

Fig. 4. Left: scalp topographies for subjects *aw* and *cv*, one of the selected CSP filters. Right: spectra for the spatially filtered signals with color coded r^2-values for the difference between the two classes below. These plots exemplary show for two subjects that CSP filter improves the discriminability of the two conditions compared to the best Laplacian filtered channel substantially (cf. Fig. 3).

shows for subject *aa* the selected filters. In Fig. 5 the corresponding classifier output signal is plotted averaged classwise over all trials of the calibration measurement. Note that this signal is much smoother and shows better discrimination than the corresponding envelope curve from the best Laplacian filtered channel (cf. Fig. 3).

The paper (Pfurtscheller et al., 1999) reports in a visually cued motor imagery paradigm similar to the one used here an early discriminatory information. In two subjects discrimination was significant about 500 ms and in one subject as early as 250 ms after cue presentation. A more detailed analysis revealed that in this subject the very early discrimination was based on short-lasting β bursts localized over the ipsilateral hand area. A detailed analysis of the early period after cue presentation in our data showed for several subjects significant discrimination about 500 ms after cue presentation but these were in none of the subjects owed to bursts in the β band.

Feedback performance

Each feedback session consisted of several runs with 25 targets each. Between two successive runs there was a short break. The number of runs performed were different for each subject and feedback. The subjects performed 6 to 8 runs of position controlled cursor, 8 runs of rate controlled cursor, and between 4 and 9 runs of the basket game. As performance measure, Wolpaw et al. (2000) suggested the information transfer rate, a measure based on information theory: the interface is modeled as a communication channel with noise (classification error) where the transmitter (the human) has to add redundancy such that a received decision can be achieved with an arbitrarily small probability of errors. With the confusion matrix $P=(p_{i,j})_{i,j}=1,\ldots,N$ ($p_{i,j}$ describes the probability to receive j while i was desired) the formula for the ITR per decision is given by $I_d = \log_2 N + \frac{1}{N}\Sigma_{i,j}p_{i,j}\log_2 p_{i,j}$. Consequently the ITR per time is defined by $I := fI_d$ with f as decision rate. For simplification we assume that $p_{i,i}=p$ and $p_{i,j}=\frac{1-p}{N-1}$ for all i,j. Then we get $I_d = \log_2 N + p\log_2 p + (1-p)\log_2\frac{1-p}{N-1}$. Note that the assumption $p_{ij}=p_{ji}(i\neq j)$ is problematic for the basket feedback, since neighboring targets are more likely to be hit accidentally. However, an estimation of the confusion matrix based on the given basket feedback data is too imprecise so that we prefer to use the simplification with a more robust estimation of the classification accuracy.
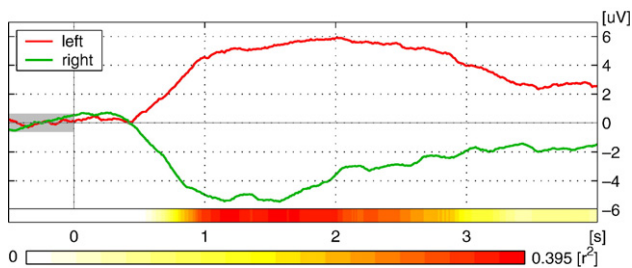

Fig. 5. Output signal averaged classwise over all trials of the calibration measurement for subject *aa*. The output is the linear combination (calculated by an LDA classifier) of the log band power estimates in the two channels obtained from the CSP filters which are displayed in Fig. 2.

Table 1
Information transfer rates (ITR) obtained in the feedback sessions measured in bits per minute as obtained by Shannon's formula

Subject/ cls	Training acc [%]	Position controlled cursor		Rate controlled cursor		Basket game	
		Overall	Peak	Overall	Peak	Overall	Peak
zq: LR	95.2	9.4	18.3	17.8	23.4	0.3	0.9
ay: LR	97.6	13.4	21.1	22.6	31.5	16.4	35.0
aa: LR	78.2	8.9	15.5	17.4	37.1	6.6	9.7
zv: LF	91.7	4.4	6.0	4.0	8.8	0.9	2.7
cv: LF	88.9	5.0	8.7	9.9	14.4	0.3	0.9
al: LF	98.0	12.7	20.3	24.4	35.4	9.6	16.1
av: LF	78.1	7.9	13.1	9.0	24.5	6.0	8.8
aw: RF	95.4	7.1	15.1	5.9	11.0	2.6	5.5
zk: RF	96.6	4.2	9.1	4.6	12.7	1.2	3.7
au: –	64.6	–	–	–	–	–	–
Mean	88.4	8.1	14.1	12.8	22.1	4.9	9.3

For each feedback session the first column ('overall') reports the average ITR of all runs, while the second column ('peak') reports the ITR of the best run. Subject au did not achieve BCI control (not used for calculating the mean). For the other 9 subjects the two letter code after the subject number indicates which movement imagery classes have been used for feedback.

Table 1 summarizes the information transfer rates that were obtained by the 9 successful subjects in the three feedback sessions. Highest ITRs were obtained in the 1D rate controlled cursor scenario.

One point that is to our knowledge special about the BBCI is that it can be operated at a high decision speed, not only theoretically, but also in practice. In the position controlled cursor, the average trial duration was 3.9 ± 1.4 s (intra-subject averages range 2.1–6.3 s), and in rate controlled cursor it was 2.8 ± 0.8 s (intra-subject averages range 1.7–3.8 s). In the basket feedback the trial duration is constant (synchronous protocol) but was individually selected by each subject with an average of 3.1 ± 0.7 (range 2.1–4.0 s). As trial duration we count the whole trial-to-trial interval including the break after target hit and before the start of the next trial. The fastest subject was aa which performed at an average speed of one decision every 1.7 s in the rate controlled cursor feedback. The most reliable performance was achieved by subject *al*: only 2% of the total 200 trials in the relative cursor control were misclassified at an average speed of one decision per 2.1 s.

Impact of previous feedback sessions

We claim that the BBCI approach can start in principle without subject training at an instantaneously high level of efficiency. To this end we engaged staff members as subjects in this study who were available for serial recording sessions: Thus, most subjects had one or more sessions of BBCI feedback that were also used to develop and stepwise optimize the system with on-line experiments before the systematic study reported in full here. Importantly, we can demonstrate that these repeated encounters with the BBCI, which might be expected to convey 'training' effects, only had a minor influence on performance. While we cannot compare feedback performances directly since the system was in development over the preceding sessions, with different kinds of feedback having been tested and continuously optimized, we could utilize the
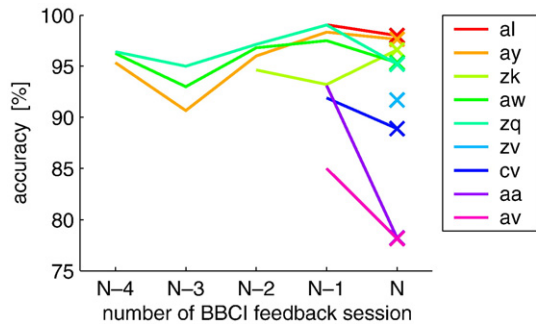
Fig. 6. Classification accuracy by cross-validation of the calibration measurements of the current study ('session N' of the full study reported here is marked by crosses) and of calibration measurements of previous BCI sessions (if any).

classification accuracy in the calibration measurements of previous sessions for comparison with the present study in order to gain insight into a possible shaping of brain responses by BBCI experiences (cf. Fig. 6). For most subjects no significant trend over time is discernible. Data of subjects *aa* and *av* could be discriminated even slightly worse in the last session reported here. Note, however, that the feedback performance of these subjects was quite well (cf. Table 1). Subject *zk* performed also in several sessions with a different feedback system which are not shown here (data were not available for analysis).

Investigating the failure

In subject *au* no features were found that enabled a reliable discrimination between any of the three motor imagery conditions. The spectra and log band power topography of the whole calibration measurement, which is shown in Fig. 7, does not reveal any significant differences when compared to the successful BCI subjects in Fig. 3, in particular no general slowing indicative of potential vigilance problems, or focal slowings related to hitherto unknown regional dysfunctions. However, the spectra from Laplacian filtered channels over sensorimotor areas exhibit almost no peak in the alpha or beta frequency range (cf. Fig. 7). Thus, no sensorimotor idle rhythm was detectable in scalp EEG that could undergo desynchronization during motor imagery. After recognizing the failure of imagery-based BCI in this subject, we added a second control calibration measurement on the same day, but now with executed movements. These recordings gave results indistinguishable from the imagery condition (data not shown).

Therefore it is likely that the BCI failure in this subject was not related to an unfavorable mental strategy (e.g., visual instead of kinesthetic; see Neuper et al., 2005), but rather that the idiosyncratic properties of the sensorimotor brain rhythms (or what is discernible of them in scalp EEG) is unsuitable for ERD/ERS-based BCI approaches.

The problem of 'BCI illiteracy' is important and challenging. Since this phenomenon is reported from all BCI laboratories it seems not be a problem of data analysis but rather inherent in the neurophysiological properties of the EEG in some subjects. An investigation of this issue will require a large experimental approach which is beyond the scope of this study.

Investigating the dependency of BCI control

It is in principle possible to voluntarily modulate sensorimotor rhythms without concurrent EMG activity (cf. Vaughan et al., 1998). Nevertheless it has to be checked for every BCI experiment involving healthy subjects. For this reason we always record EMG signals even though they are not used in the online system. On one hand we investigated classwise averaged spectra, their statistical significant differences, and the scalp distributions and time courses of the energy of the μ and β rhythm. The results substantiated that differences of the motor imagery classes indeed were located in sensorimotor cortices and had the typical time courses (except for subject *au* in whom no consistent differences were found). On the other hand we compared how much variance of the classifier output and how much variance of the EMG signals can be explained by the target class. Much in the spirit of Vaughan et al. (1998), we made the following analysis using the squared bi-serial correlation coefficient r^2 (see Methodological and technical details). The r^2-value was calculated for the classifier output and for the band-pass filtered and rectified EMG signals of the feedback sessions. Then the maximum of those time series was determined resulting in one r^2-value per subject and feedback session for EMG resp. for the BCI classifier signal. The r^2 for EMG was in the range 0.01 to 0.08 (mean 0.03 ± 0.02) which is very low compared to the r^2 for the BCI classifier signal which was in the range 0.20 to 0.79 (mean 0.46 ± 0.16). The fact that the BBCI works without being dependent on eye movements or visual input was additionally verified by letting two subjects control the BBCI with closed eyes (targets provided acoustically) which resulted in a comparable performance as in the closed loop feedback (100% hits for subject *al* and 96% hits for subject *ay*). An important advantage is that when using the BBCI the subject is free to scan the visual environment by exploratory eye movements without diminishing the BBCI efficiency.
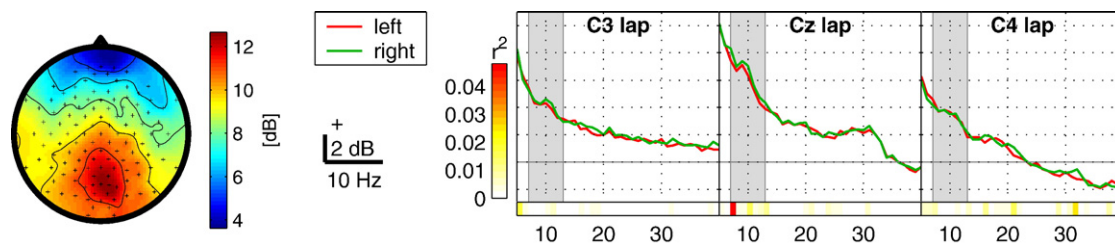

Fig. 7. Left: log band power topography averaged over the calibration measurement of subject *au*. Right: spectra during left vs. right hand motor imagery in three Laplacian filtered channels over sensori motor areas. Compared to the successful subjects almost no peak in the alpha or in the beta frequency range is visible. The low r^2-values show that no discriminatory information is found with respect to band power.

Discussion

The Berlin Brain–Computer Interface makes use of a machine learning approach towards BCI. Working with high dimensional, complex features obtained from 128 channel EEG allows the system a distinct flexibility for adapting to the individual characteristics of each user's brain. The result from a feedback study with 10 subjects demonstrates that the BBCI system (1) robustly transfers the discrimination of mental states from the calibration to the feedback sessions, (2) allows a very fast switching between mental states, and (3) provides reliable feedback directly after a short calibration measurement and machine learning without the need that the subject adapts to the system (all at high information transfer rates, see Table 1).

Although this study involving 10 subjects gives a clear indication of the qualities of the proposed system, extended studies need to be performed to investigate how general they are with respect to different groups of subjects. It is of particular interest to verify how BBCI works for paralyzed patients. A positive result was obtained by Kübler et al. (2005) where it has been demonstrated that ALS patients can indeed operate a BCI by the voluntary control of sensorimotor rhythms, which is a requirement for the direct transfer of the proposed system to patient use. A crucial open issue is, how the BBCI feature of minimal subject training transfers to patients.

Other recent BBCI lines of research comprise (a) mental typewriter experiments (Müller and Blankertz, 2006; Blankertz et al., 2006b), (b) the online use of the error potential, (c) investigation of synchronization features that capture dynamic interactions of brain areas (Meinecke et al., 2005; Nolte et al., 2006) for BCI, and (d) general real-time single-trial EEG analysis in more natural paradigms, e.g., in driving situations (Dornhege et al., 2007a).

Our future studies will strive for 2D cursor control and robot arm control (Popescu et al., 2006), still maintaining our philosophy of minimal or no subject training and non-invasiveness.

Acknowledgments

References

Berger, H., 1933. Über das Elektroenkephalogramm des Menschen. Arch. Psychiatr. Nervenkrankh. 99 (6), 555–574.

Birbaumer, N., Kübler, A., Ghanayim, N., Hinterberger, T., Perelmouter, J., Kaiser, J., Iversen, I., Kotchoubey, B., Neumann, N., Flor, H., 2000. The though translation device (TTD) for completely paralyzed patients. IEEE Trans. Rehabil. Eng. 8 (2), 190–193 (June).

Blankertz, B., Dornhege, G., Schäfer, C., Krepki, R., Kohlmorgen, J., Müller, K.-R., Kunzmann, V., Losch, F., Curio, G., 2003. Boosting bit rates and error detection for the classification of fast-paced motor commands based on single-trial EEG analysis. IEEE Trans. Neural Syst. Rehabil. Eng. 11 (2), 127–131.

Blankertz, B., Müller, K.-R., Curio, G., Vaughan, T.M., Schalk, G., Wolpaw, J.R., Schlögl, A., Neuper, C., Pfurtscheller, G., Hinterberger, T., Schröder, M., Birbaumer, N., 2004. The BCI competition 2003: progress and perspectives in detection and discrimination of EEG single trials. IEEE Trans. Biomed. Eng. 51 (6), 1044–1051.

Blankertz, B., Dornhege, G., Krauledat, M., Müller, K.-R., Kunzmann, V., Losch, F., Curio, G., 2006a. The Berlin Brain–Computer Interface: EEG-based communication without subject training. IEEE Trans. Neural Syst. Rehabil. Eng. 14 (2), 147–152.

Blankertz, B., Dornhege, G., Krauledat, M., Schröder, M., Williamson, J., Murray-Smith, R., Müller, K.-R., 2006b. The Berlin Brain–Computer Interface presents the novel mental typewriter Hex-o-Spell. Proceedings of the 3rd International Brain–Computer Interface Workshop and Training Course 2006. Verlag der Technischen Universität Graz, pp. 108–109.

Blankertz, B., Dornhege, G., Lemm, S., Krauledat, M., Curio, G., Müller, K.-R., 2006c. The Berlin Brain–Computer Interface: machine learning based detection of user specific brain states. J. Univer. Comput. Sci. 12 (6), 581–607.

Blankertz, B., Müller, K.-R., Krusienski, D., Schalk, G., Wolpaw, J.R., Schlögl, A., Pfurtscheller, G., del Millán, J.R., Schröder, M., Birbaumer, N., 2006d. The BCI competition III: validating alternative approaches to actual BCI problems. IEEE Trans. Neural Syst. Rehabil. Eng. 14 (2), 153–159.

Cheng, M., Gao, X., Gao, S., Xu, D., 2002. Design and implementation of a brain–computer interface with high transfer rates. IEEE Trans. Biomed. Eng. 49 (10), 1181–1186.

Curran, E.A., Stokes, M.J., 2003. Learning to control brain activity: a review of the production and control of EEG components for driving brain–computer interface (BCI) systems. Brain Cogn. 51, 326–336.

da Silva, F.H., van Lierop, T.H., Schrijer, C.F., van Leeuwen, W.S., 1973. Organization of thalamic and cortical alpha rhythm: spectra and coherences. Electroencephalogr. Clin. Neurophysiol. 35, 627–640.

del Millán, J.R., Mouriño, J., 2003. Asynchronous bci and local neural classifiers: an overview of the adaptive brain interface project. IEEE Trans. Neural Syst. Rehabil. Eng. 11 (2), 159–161.

del Millán, J.R., Mouriño, J., Franzé, M., Cinotti, F., Varsta, M., Heikkonen, J., Babiloni, F., 2002. A local neural classifier for the recognition of EEG patterns associated to mental tasks. IEEE Trans. Neural Netw. 13 (3), 678–686.

Dornhege, G., Blankertz, B., Curio, G., Müller, K.-R., 2004a. Boosting bit rates in non-invasive EEG single-trial classifications by feature combination and multi-class paradigms. IEEE Trans. Biomed. Eng. 51 (6), 993–1002 (June).

Dornhege, G., Blankertz, B., Curio, G., Müller, K.-R., 2004b. Increase information transfer rates in BCI by CSP extension to multi-class. In: Thrun, S., Saul, L., Schölkopf, B. (Eds.), Advances in Neural Information Processing Systems, vol. 16. MIT Press, Cambridge, MA, pp. 733–740.

Dornhege, G., Blankertz, B., Krauledat, M., Losch, F., Curio, G., Müller, K.-R., 2006. Combined optimization of spatial and temporal filters for improving brain–computer interfacing. IEEE Trans. Biomed. Eng. 53 (11), 2274–2281.

Dornhege, G., Braun, M., Kohlmorgen, J., Blankertz, B., Müller, K.-R., Curio, G., Hagemann, K., Bruns, A., Schrauf, M., Kincses, W., 2007a. Improving human performance in a real operating environment through real-time mental workload detection. In: Dornhege, G., del Millán, J.R., Hinterberger, T., McFarland, D., Müller, K.-R. (Eds.), Towards Brain–Computer Interfacing. MIT Press, pp. 409–422.

Dornhege, G., del Millán, J.R., Hinterberger, T., McFarland, D., Müller, K.-R. (Eds.), 2007b. Towards Brain–Computer Interfacing. MIT Press.

Dornhege, G., Krauledat, M., Müller, K.-R., Blankertz, B., 2007c. Towards Brain–Computer Interfacing, chapter General signal processing and machine learning tools for BCI. MIT Press, pp. 207–233.

Elbert, T., Rockstroh, B., Lutzenberger, W., Birbaumer, N., 1980. Biofeedback of slow cortical potentials. I. Electroencephalogr. Clin. Neurophysiol. 48, 293–301.

Fukunaga, K., 1990. Introduction to statistical pattern recognition, 2nd edition. Academic Press, Boston.

Guger, C., Ramoser, H., Pfurtscheller, G., 2000a. Real-time EEG analysis with subject-specific spatial patterns for a Brain Computer Interface (BCI). IEEE Trans. Neural Syst. Rehabil. Eng. 8 (4), 447–456.

Guger, C., Ramoser, H., Pfurtscheller, G., 2000b. Real-time EEG analysis with subject-specific spatial patterns for a Brain Computer Interface (BCI). IEEE Trans. Neural Syst. Rehabil. Eng. 8 (4), 447–456.

Haykin, S.S., 1995. Adaptive Filter Theory. Prentice Hall.

Jasper, H., Andrews, H.L., 1938. Normal differentiation of occipital and precentral regions in man. Arch. Neurol. Psychiatry (Chicago) 39, 96–115.

Jasper, H., Penfield, W., 1949. Electrocorticograms in man: effects of voluntary movement upon the electrical activity of the precentral gyrus. Arch. Psychiatr. Nervenkrankh. 183, 163–174.

Kaper, M., Ritter, H., 2004. Generalizing to new subjects in brain–computer interfacing. Proceedings of the 26th Annual International Conference IEEE EMBS, San Francisco, pp. 4363–4366.

Koles, Z.J., Soong, A.C.K., 1998. EEG source localization: implementing the spatio-temporal decomposition approach. Electroencephalogr. Clin. Neurophysiol. 107, 343–352.

Krauledat, M., Losch, F., Curio, G., 2006. Brain state differences between calibration and application session influence BCI classification accuracy. Proceedings of the 3rd International Brain–Computer Interface Workshop and Training Course 2006. Verlag der Technischen Universität Graz, pp. 60–61.

Krausz, G., Scherer, R., Korisek, G., Pfurtscheller, G., 2003. Critical decision-speed and information transfer in the "Graz Brain–Computer Interface". Appl. Psychophysiol. Biofeedback 28 (3), 233–240.

Kübler, A., Kotchoubey, B., Kaiser, J., Wolpaw, J., Birbaumer, N., 2001. Brain–computer communication: unlocking the locked in. Psychol. Bull. 127 (3), 358–375.

Kübler, A., Nijboer, F., Mellinger, J., Vaughan, T.M., Pawelzik, H., Schalk, G., McFarland, D.J., Birbaumer, N., Wolpaw, J.R., 2005. Patients with ALS can use sensorimotor rhythms to operate a brain–computer interface. Neurology 64 (10), 1775–1777.

Lemm, S., Blankertz, B., Curio, G., Müller, K.-R., 2005. Spatio-spectral filters for improved classification of single trial EEG. IEEE Trans. Biomed. Eng. 52 (9), 1541–1548.

McFarland, D.J., Sarnacki, W.A., Wolpaw, J.R., 2003. Brain–computer interface (BCI) operation: optimizing information transfer rates. Biol. Psychol. 63, 237–251.

Meinecke, F.C., Ziehe, A., Kurths, J., Müller, K.-R., 2005. Measuring phase synchronization of superimposed signals. Phys. Rev. Lett. 94 (8), 084102.

Müller, K.-R., Blankertz, B., 2006. Toward noninvasive brain–computer interfaces. IEEE Signal Process. Mag. 23 (5), 125–128 (September).

Müller, K.-R., Mika, S., Rätsch, G., Tsuda, K., Schölkopf, B., 2001. An introduction to kernel-based learning algorithms. IEEE Neural Netw. 12 (2), 181–201 (May).

Müller, K.-R., Anderson, C.W., Birch, G.E., 2003. Linear and non-linear methods for brain–computer interfaces. IEEE Trans. Neural Syst. Rehabil. Eng. 11 (2), 165–169.

Müller, K.-R., Krauledat, M., Dornhege, G., Curio, G., Blankertz, B., 2004. Machine learning techniques for brain–computer interfaces. Biomed. Tech. 49 (1), 11–22.

Neuper, C., Pfurtscheller, G., 2001. Event-related dynamics of cortical rhythms: frequency-specific features and functional correlates. Int. J. Psychophysiol. 43, 41–58.

Neuper, C., Scherer, R., Reiner, M., Pfurtscheller, G., 2005. Imagery of motor actions: differential effects of kinesthetic and visual-motor mode of imagery in single-trial EEG. Brain Res. Cogn. Brain Res. 25 (3), 668–677.

Nolte, G., Meinecke, F.C., Ziehe, A., Müller, K.-R., 2006. Identifying interactions in mixed and noisy complex systems. Phys. Rev. E 73.

Pfurtscheller, G., Lopes da Silva, F.H., 1999. Event-related EEG/MEG synchronization and desynchronization: basic principles. Clin. Neurophysiol. 110 (11), 1842–1857 (Nov.).

Pfurtscheller, G., Neuper, C., Ramoser, H., Müller-Gerking, J., 1999. Visually guided motor imagery activates sensorimotor areas in humans. Neurosci. Lett. 269, 153–156.

Pfurtscheller, G., Neuper, C., Birbaumer, N., 2005. Human brain–computer interface. In: Riehle, A., Vaadia, E. (Eds.), Motor Cortex in Voluntary Movements. CRC Press, New York, pp. 367–401. chapter 14.

Pfurtscheller, G., Brunner, C., Schlögl, A., Lopes da Silva, F.H., 2006. Mu rhythm (de)synchronization and EEG single-trial classification of different motor imagery tasks. NeuroImage 31 (1), 153–159.

Popescu, F., Badower, Y., Fazli, S., Dornhege, G., Müller, K.-R., 2006. EEG-based control of reaching to visual targets. In: Ijspeert, A.J., Buchli, J., Selverston, A., Rabinovich, M., Hasler, M., Gerstner, W., Billard, A., Markram, H., Floreano, D. (Eds.), Dynamical Principles for Neuroscience and Intelligent Biomimetic Devices—Abstracts of the EPFL-LATSIS Symposium 2006, pp. 123–124. Lausanne.

Ramoser, H., Müller-Gerking, J., Pfurtscheller, G., 2000. Optimal spatial filtering of single trial EEG during imagined hand movement. IEEE Trans. Rehabil. Eng. 8 (4), 441–446.

Rockstroh, B., Birbaumer, N., Elbert, T., Lutzenberger, W., 1984. Operant control of EEG and event-related and slow brain potentials. Biofeedback Self-Regul. 9 (2), 139–160.

Shenoy, P., Krauledat, M., Blankertz, B., Rao, R.P.N., Müller, K.-R., 2006. Towards adaptive classification for BCI. J. Neural Eng. 3, R13–R23.

Tomioka, R., Dornhege, G., Aihara, K., Müller, K.-R., 2006. An iterative algorithm for spatio-temporal filter optimization. Proceedings of the 3rd International Brain–Computer Interface Workshop and Training Course 2006. Verlag der Technischen Universität Graz, pp. 22–23.

Tomioka, R., Aihara, K., Müller, K.-R., in press. Logistic regression for single trial EEG classification. In: Advances in Neural Inf. Proc. Systems (NIPS 06), volume 19. MIT Press.

Vaughan, T.M., Miner, L.A., Wolpaw, J.R., 1998. EEG-based communication: analysis of concurrent EMG activity. Electroencephalogr. Clin. Neurophysiol. 107, 428–433.

Wolpaw, J.R., Birbaumer, N., William, J., Heetderks, D.J., McFarland, P., Peckham, H., Schalk, G., Donchin, E., Quatrano, L.A., Robinson, C.J., Vaughan, T.M., 2000. Brain–computer interface technology: a review of the first international meeting. IEEE Trans. Rehabil. Eng. 8 (2), 164–173.

Wolpaw, J.R., Birbaumer, N., McFarland, D.J., Pfurtscheller, G., Vaughan, T.M., 2002. Brain–computer interfaces for communication and control. Clin. Neurophysiol. 113, 767–791.